

AD-A140 794

DETECTION OF SOLAR GRAVITY MODE OSCILLATIONS(U)  
STANFORD UNIV CA CENTER FOR SPACE SCIENCE AND  
ASTROPHYSICS P H SCHERRER 01 NOV 83 CSSA-ASTRO-84-03  
N00014-76-C-0207

1/1

UNCLASSIFIED

F/G 3/2

NL



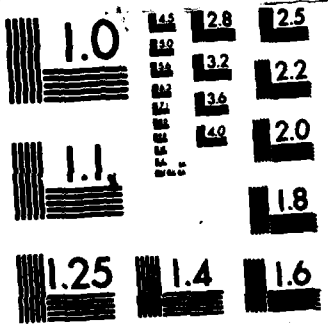
END

DATE

FILMED

16 APR 84

DTIC



MICROCOPY RESOLUTION TEST CHART  
NATIONAL BUREAU OF STANDARDS-1963-A

**DETECTION OF SOLAR GRAVITY MODE OSCILLATIONS**

by

**Philip H. Scherrer**

**CSSA-ASTRO-84-03**

**November 1, 1983**

①

DETECTION OF SOLAR GRAVITY MODE OSCILLATIONS

by

Philip H. Scherrer

CSSA-ASTRO-84-03

November 1, 1983

Submitted to:  
Proceedings of Solar Seismology From Space  
A Conference at Snowmass, Colorado sponsored by NASA and JPL  
August 17-19, 1983

OFFICE OF NAVAL RESEARCH  
Contract N00014-76-C-0207

NATIONAL AERONAUTICS AND SPACE ADMINISTRATION  
Grant NGR05-020-559  
Contract NAS5-24420

NATIONAL SCIENCE FOUNDATION  
Atmospheric Sciences Section  
Grant ATM77-20580

Max C. Fleischmann Foundation

DTIC  
ELECTE  
S MAY 4 1984 D  
A

REPORT DOCUMENTATION PAGE		READ INSTRUCTIONS BEFORE COMPLETING FORM	
1. REPORT NUMBER CSSA-ASTRO-84-03	2. GOVT ACCESSION NO. AD-A140794	3. RECIPIENT'S CATALOG NUMBER	
4. TITLE (and Subtitle) Detection of Solar Gravity Mode Oscillations		5. TYPE OF REPORT & PERIOD COVERED Scientific; Technical	
7. AUTHOR(s) Philip H. Scherrer		6. PERFORMING ORG. REPORT NUMBER	
8. PERFORMING ORGANIZATION NAME AND ADDRESS Center for Space Science and Astrophysics Stanford University Stanford, California 94305		9. CONTRACT OR GRANT NUMBER(s) N00014-76-C-0207	
11. CONTROLLING OFFICE NAME AND ADDRESS Office of Naval Research Electronics Program Office Arlington, Virginia 22217		10. PROGRAM ELEMENT, PROJECT, TASK AREA & WORK UNIT NUMBERS	
14. MONITORING AGENCY NAME & ADDRESS (if different from Controlling Office)		12. REPORT DATE November 1983	
		13. NUMBER OF PAGES 10	
		15. SECURITY CLASS. (of this report)	
		15a. DECLASSIFICATION/DOWNGRADING SCHEDULE	
16. DISTRIBUTION STATEMENT (of this Report) This document has been approved for public release and sale; its distribution is unlimited.			
17. DISTRIBUTION STATEMENT (of the abstract entered in Block 20, if different from Report)			
18. SUPPLEMENTARY NOTES			
19. KEY WORDS (Continue on reverse side if necessary and identify by block number) Solar Oscillations G-Modes			
20. ABSTRACT (Continue on reverse side if necessary and identify by block number) An analysis of solar velocity data obtained at the Stanford Solar Observatory has shown the existence of solar global oscillations (Delache and Scherrer, Nature, in press). The oscillations are in the range of 45 to 105 $\mu$ Hz (160 to 370 minutes) and are interpreted as internal gravity modes of degree $l=1$ and $l=2$ . <i>minchy</i>			

**DTIC  
SELECTED**  
MAY 4 1984

A

# DETECTION OF SOLAR GRAVITY MODE OSCILLATIONS

Philip H. Scherrer

Center for Space Science and Astrophysics  
Stanford University, ERL  
Stanford, California 94305 - U.S.A.

5010  
COPY  
RESPECTED  
2

Session For  
GRA&I  
TAB  
Announced  
Classification

By  
Distribution/  
Availability Codes

Dist	Avail and/or Special
Al	

## Abstract

An analysis of solar velocity data obtained at the Stanford Solar Observatory has shown the existence of solar global oscillations (Delache and Scherrer, Nature, in press). The oscillations are in the range 45 to 105  $\mu\text{Hz}$  (180 to 370 minutes) and are interpreted as internal gravity modes of degree  $l=1$  and  $l=2$ .

## The Data

Observations of the global solar velocity field have been recorded at the Stanford Solar Observatory since 1976. These observations have recently been examined for long period oscillations at periods other than 180 minutes. Delache and Scherrer (1983) have reported the results of this analysis. This report will review that work and expand on the methods used to find significant peaks in the power spectrum in the presence of noise and gaps in the data.

Scherrer and Wilcox (1983) have described the observing procedures and preliminary data reduction applied to the observations. The observations are differential measures of the line-of-sight velocity of the solar surface. They are made by comparing the average doppler shift from the center of the solar disk with the doppler shift from a concentric annulus. Since it appeared that interesting features were present in the low frequency part of the spectrum, the computation was extended down to  $\nu=0$ . Since only the low frequency part of the spectrum is examined here, the data was averaged into 5-minute intervals and normalized within each day as in the previous analysis.

First the Fourier transform of the 4 years of Stanford data (1977-1980) was computed using a standard fast Fourier transform code (FFT). It was found that the largest power is in the range 45  $\mu\text{Hz}$  - 105  $\mu\text{Hz}$  (about 180 to 370 minutes). The resulting power spectrum shows a number of sets of lines with separations corresponding to day side bands (i.e. 11.57  $\mu\text{Hz}$ ) which obviously come from the nightly gaps in the data. Comparing the 4-year spectrum with individual yearly spectra, it was found that the strongest lines were more prominent in 1979 than in the other years. This may be due to the relatively clear skies and the distribution of observing times in 1979. As a first step, the analysis was restricted to that year. Figure 1a shows the 1979 spectrum. The observations were begun on 7 April and

continued through 23 July with most of the data collected in late May through July. There were a total of 240 hours of data available. As described in the previous report (Scherrer and Wilcox, 1983) the data were scaled for each observing run to have the same daily variance. The daily normalization factor used is highly correlated to the integrated signal power in the 5-minute band, suggesting that the variations in power are due to instrumental changes. Although the analysis was done using this daily normalized data, the results were rescaled using the average normalizing factor to provide an approximate scale in m/s. This normalization has both desired and undesired effects. It allows combining data from different years and from different observation sets where the raw data shows jumps in average signal due to variations in the instrument with time and to variations in the preliminary data reduction procedures. This method also removes apparent sensitivity changes that may result from variations in solar activity. The main structure of the spectrum is the same for both the normalized and raw data, so the normalized data were used to allow direct comparisons with different intervals of time.

#### *Significance of Spectrum*

An estimate of the number of peaks in the spectrum that are significantly above the noise can be made by examining the cumulative distribution of the spectrum. A power spectrum computed from a normally distributed noise source will have an exponential distribution, thus the logarithm of the cumulative distribution will decrease linearly with power. A departure from a straight line is an indication

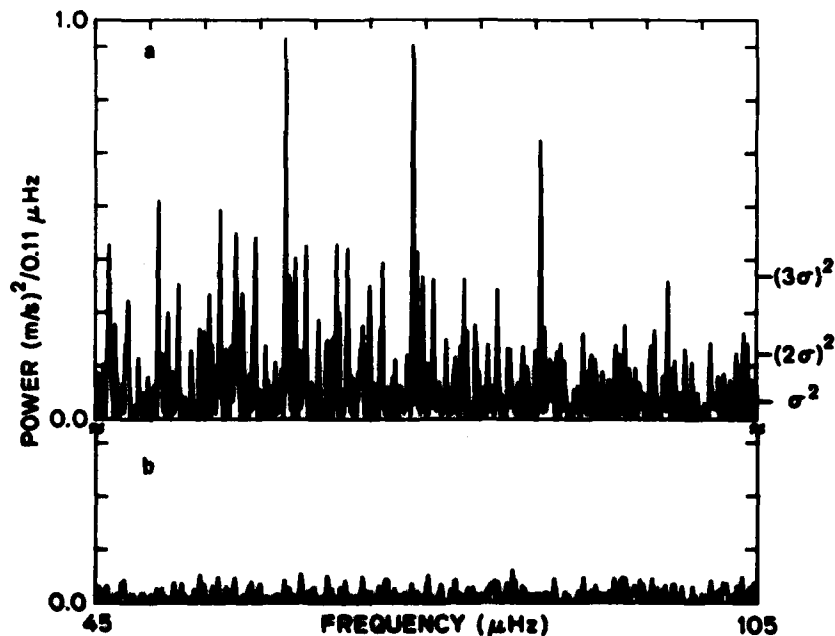


Figure 1. The power spectrum of velocity observations from the Stanford Solar Observatory in 1979. The spectrum in the range 45-105  $\mu\text{Hz}$  (300 to 180 minutes) is shown. Part (a) shows the original spectrum, part (b) shows the spectrum to the same scale after fourteen peaks were identified and the associated sinusoidal waves subtracted from the data. The scale shown has been corrected for the average normalizing factor. From Delache and Scherrer (1983).

of the presence of significant spectral features and the slope of the line is a measure of the variance ( $\sigma^2$ ) in the spectrum.

Figure 2 shows this plot for the 45-105  $\mu\text{Hz}$  range of the 1979 spectrum. The actual data is represented by large dots. The smaller points are for a spectrum computed the same way from data constructed by taking the original data for each day in reversed order, thus keeping the original window function. Any coherent signal present in the original data will be eliminated by this procedure. The noise statistics for the modified data power spectrum should be unchanged for periods up to the average daily observing time, i.e. for frequencies higher than 40  $\mu\text{Hz}$ . It can be seen that in the actual data there are more peaks with value above  $0.25 (m/s)^2$  than in the reversed data. The level at which the actual distribution begins to depart from the noise distribution is around  $2.5 \sigma$ . Since the spectrum was computed with a resolution of 0.02  $\mu\text{Hz}$  but has a natural resolution of only 0.11  $\mu\text{Hz}$ , there will be about five points shown for each significant peak in the spectrum. Also, since the data has gaps at night, the day sidelobe structure introduces 2 to 4 apparently significant artificial peaks for each true peak. This reduces the number of independent spectral estimates to about 200. These considerations suggest that there are about 10 independent peaks above the  $2.5 \sigma$  level.

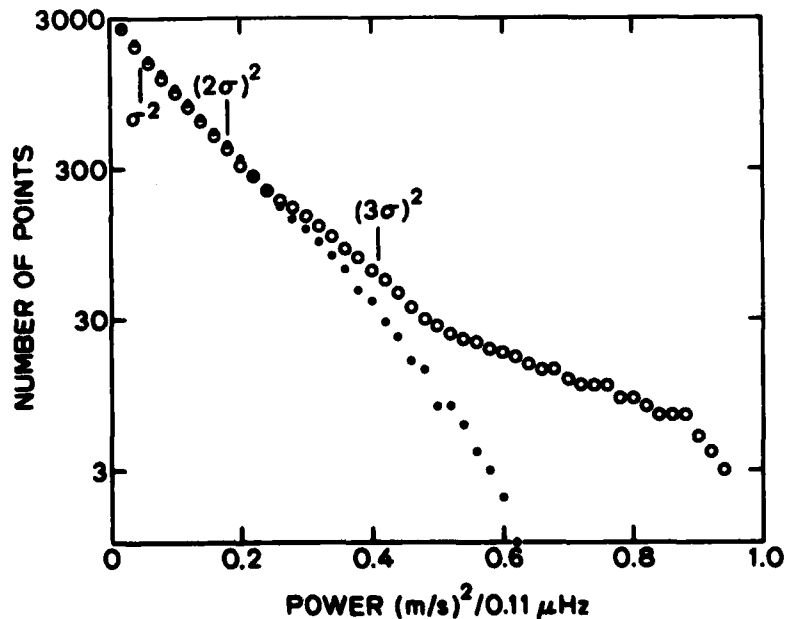


Figure 2. The cumulative distribution function of the spectrum in Figure 1a. The log of the number of spectral estimates with size larger than a given value is plotted vs that value. The large dots correspond to the observed spectrum. The small dots are from a similar spectrum computed with the data within each day taken in reversed order. The small dots then refer to a spectrum with the same window and noise characteristics but no coherent oscillations. The variance which is deduced from the slope is  $\sigma^2 = (20 \text{ cm/s})^2$ .

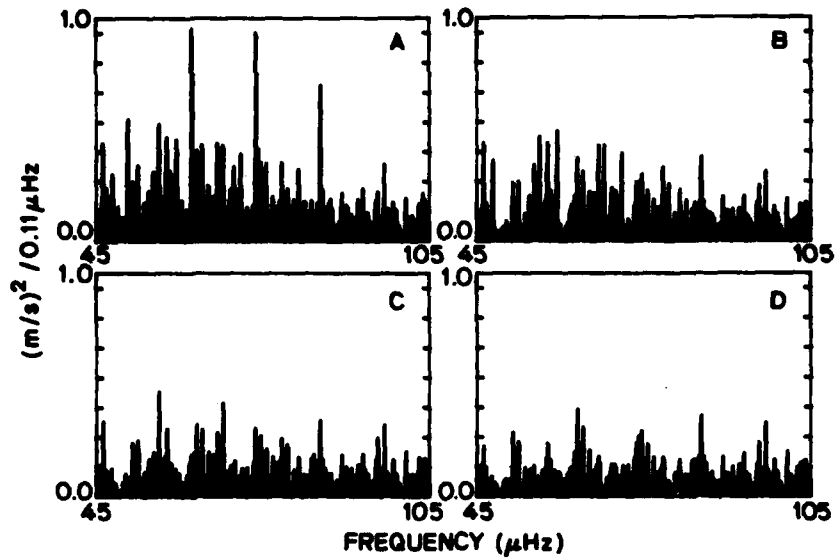


Figure 3. The spectrum of the original data (a), the spectrum after removing the largest peak (b), after removing the second peak (c), and after removing the third peak (d). (from Scherrer, 1983).

freq. $\mu Hz$	period min	power $(m/s)^2$	$l$	$n$
58.25	286.1	0.15	1	10
59.52	280.0	0.52	1	10
64.13	259.9	0.17	1	9
65.30	255.2	0.22	1	9
73.43	227.0	0.18	1	8
*73.84	225.7	0.98	1	8
83.50	199.6	0.09	1	7
95.70	174.1	0.23	1	6
96.94	171.9	0.31	1	6
*50.72	328.6	0.07	2	20
56.33	295.9	0.49	2	18
59.52	280.0	0.52	2	17
63.12	264.1	0.42	2	16
66.65	250.0	0.13	2	15
46.23	360.5	0.25	day/4	
62.29	267.6	0.98	-	
92.21	180.7	0.10	day/8	

Table 1. Frequencies of the 14 peaks found in the 45-105  $\mu Hz$  range of the 1979 spectrum. The frequencies are in  $\mu Hz$  with the corresponding periods shown in minutes. The power is shown as amplitude squared  $(m/s)^2$ . The classification of  $n$  and  $l$  are described in the text. The 2 peaks in marked with an asterisk are an alternate identification for the peak at 62.29  $\mu Hz$  and its associated side-lobes. Note that the peak at 59.52  $\mu Hz$  could be identified as part of either an  $l=1$  or  $l=2$  series and is included in the table twice.

### Cleaning the Spectrum

Since the spectrum appears to be dominated by the sidelobe structure from the observing times, a procedure must be performed to eliminate these sidelobes. An iterative peak removal technique was used to find and remove the peaks one at a time. First an FFT was computed and the largest peak determined. Next that peak was accurately found with a fine resolution simple Fourier transform in the vicinity of the peak. Finally the corresponding sinusoidal signal was subtracted from the original data. This procedure was repeated, producing a list of frequencies free of day sidelobes. Figure 3 shows the original spectrum and the spectrum after removing each of the first 3 peaks. It can be seen that for each peak removed, the entire

sidelobe structure is also removed. Selecting peaks with amplitudes greater than about 30 cm/s, 14 peaks were found in the frequency band 45 to 105  $\mu\text{Hz}$ . Using the same amplitude criterion, another 8 peaks were found at frequencies in the range extending to 165  $\mu\text{Hz}$ . These higher frequency peaks will not be discussed here. The list of 14 peaks is given in Table 1. Note that since the spectrum is assumed to consist of a set of line spectra, the scaling used in this paper is amplitude squared rather than power in the usual sense. To convert to the usual power spectrum scaling all values must be divided by 4 and would refer to intervals on 0.11  $\mu\text{Hz}$  (see e.g. Bath, 1974, p183).

To see the effect of removing the complete set of peaks from the original data, the spectrum of the residual data after subtracting these 22 sinusoids is shown in Figure 1b. Figure 1b is shown to the same scale as Figure 1a. It is clear that far more than 14 peaks in the band shown have been removed in the resulting spectrum. This method of peak identification appears to be a powerful tool for analysis of power spectra computed from data with complicated windows. The method finds a table of periods, phases and amplitudes that best clean the spectrum. From experiments with artificial data, we have concluded that while the correct peak is usually found, a side lobe introduced by the window is occasionally selected. This is a weakness of the procedure that requires care in examining the resulting peaks. We have also found that *the amplitudes determined from data with a complicated window are not to be relied upon.*

The method described above relies upon the single assumption that the examined signals consist of coherent sine waves. It is then not surprising that for each frequency removed, a complete day-sidelobe set of lines disappears from the spectrum. A further check is necessary to determine whether or not the signal is coherent for the full span of the observations. For that purpose, the data with the tabulated frequencies removed was divided into two parts, 7 April through 15 June and 16 June through 23 July. Figure 4 shows a set of nine spectra resulting from this division. The top row shows the original spectrum (left), the spectrum of the first half of the data (middle), and the spectrum of the last half of the data (right). A large variation in the appearance of the spectra is obvious. A first impression is that these spectra represent either very noisy data or unrelated data. Examination of the bottom two rows shows that the first impression is wrong. The second row contains the residual spectra similar to Figure 1b for each of the intervals in the top row. The middle row, left spectrum is essentially the same as Figure 1b. The center and right frames are for two halves of the interval but cleaned by subtracting the sinusoids found for the *entire* interval. The spectra of each part separately do not show any of the removed frequencies. If any of the frequencies removed were not present in both halves of the data, they would have been artificially put into the cleaned data by the subtraction of the sinusoid over the entire interval. In that case they would show in the spectrum of one or both halves of the cleaned data. This is strong evidence that the signals are all present in both halves of the observations. The bottom row demonstrates the variability in amplitude caused by the observing window. Using only the times of observations and the list of frequencies and phases found above, a cleaned dataset was reconstructed. The spectra from the entire interval and the two halves are shown in the bottom row. Note that all three frames are computed from artificial data generated from the same set of frequencies and phases. The only difference between frames on the bottom row is the observing window. The conclusion is that for windows obtained at Stanford (which are similar to the average distribution of observations in the Crimea and at SCLERA), the relative amplitudes of peaks may be dominated by interference caused by data gaps.

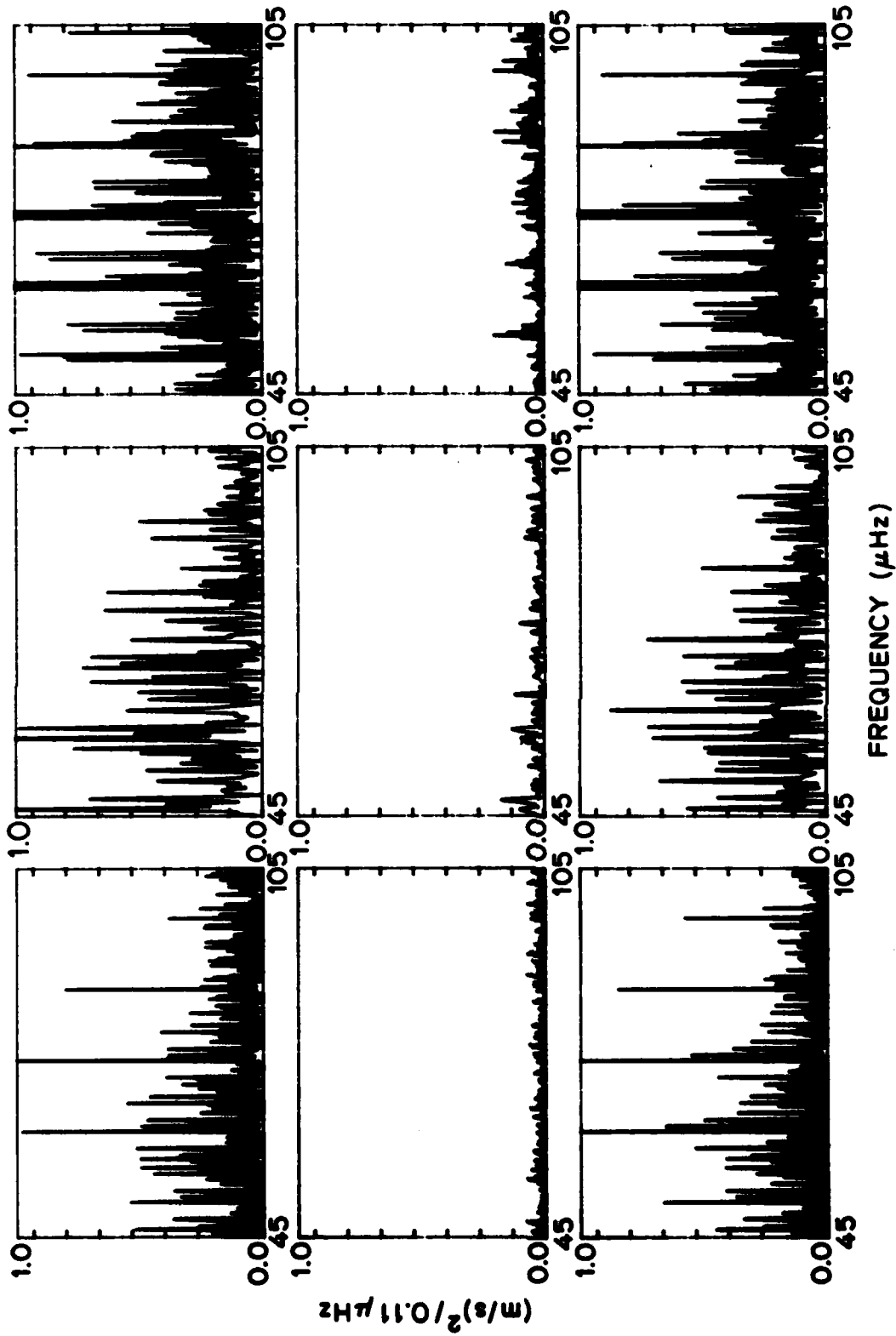


Figure 4. Spectra of the entire interval and both halves of the interval. The first column contains spectra for the entire data interval. The center column is for the first half, the right column is for the last half. The top row is the original data, the middle row is the residuals after subtracting the peaks found in the entire interval (similar to Figure 1b), and the bottom row is data reconstructed from the peak list.

### Peak Identification

Returning to table 1, two of the 14 peaks are apparently day aliases at  $1/4$  and  $1/8$  of a day. (With only 3 months of data the previously reported peak at 160.01 minutes can not be distinguished from  $1/9$  of a day and is masked by the sidelobes of the lower day-harmonics). This leaves 12 peaks for further analysis. There is some ambiguity in the true identification of the largest of the remaining peaks. The first  $1/\text{day}$  sidelobe is of the same amplitude as the main peak. This could be due to two true peaks with separation  $1/\text{day}$  or  $2/\text{day}$ . By careful examination of the peak shapes, the peak at  $62.29 \mu\text{Hz}$  has been identified as the true peak with a smaller peak at  $96.94 \mu\text{Hz}$ , although the identification could have been made as a true peak at  $73.84 \mu\text{Hz}$  with smaller peaks at  $50.72$  and  $96.94 \mu\text{Hz}$ . The alternate identifications are shown in parentheses in Table 1.

### Interpretation

In order to interpret the peaks found in this spectrum, one must seek guidance from theory. Estimates for the spacing of  $g$ -mode oscillations made from the full asymptotic approximation (Tassoul 1980) and calculated from complete solar models (Berthomieu, Provost, and Christensen-Dalsgaard, private communications) suggest that the  $g$ -mode oscillations of the same degree  $l$  should be about equally spaced in period for order large enough ( $n > 6$ ). Therefore the list of prominent peaks was examined for equal spacing in period. Three of the four largest peaks are separated in period by 15.5 minutes. This is very close to the spacing of the standard solar model for  $g$ -modes with degree two and order greater than 10.

To aid in further identification of the modes the asymptotic approximation (Tassoul 1980) is used. This approximation shows that for sufficiently large order  $n$

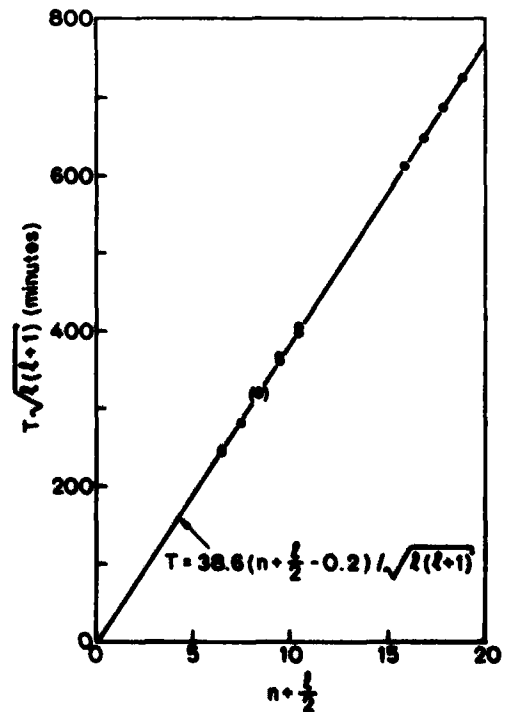


Figure 5. The observed modes are plotted within the structure of the asymptotic formula described in the text. The line is determined from the three largest peaks that have been assigned. From Delache and Scherrer (1983).

the period  $T$  is:

$$T = T_0 \left( n + \frac{l}{2} - \frac{1}{4} \right) / \sqrt{l(l+1)}$$

If the three peaks with 15.5 minute separation are part of an  $l=2$  series, then  $T_0$  and thus the probable spacing for the  $l=1$  and  $l=3$  series can be computed. Doing this, it is seen that most of the remaining peaks are likely to be part of the  $l=1$  series. Using the estimate for  $l$ , the observed periods can be plotted as  $T \sqrt{l(l+1)}$  vs  $(k + l/2 - 1/4)$  where  $k$  is an integer increasing with period. If the peaks are consistent with the model and the correct degree  $l$  has been assigned, the points will all lie on a straight line. From the intercept of this line both the best value for  $n$  and the correct value for  $-1/4$  term can be determined. This has been done in Figure 5.

The three largest peaks were used to define the  $l=2$  series and thus to find  $T_0$ . The rightmost dots in Figure 5 represent the three largest peaks which determine the  $l=2$  series. The other modes identified in Table 1 are also shown. The line was found from the three large  $l=2$  peaks only. It can be seen that the other peaks are organized in the expected  $g$ -mode structure. The  $T_0$  implied by the identified modes is  $38.8 \pm 0.5$  minutes. The intercept of the best fit line with the abscissa is expected to be 0.25 and is found to be  $0.2 \pm 0.1$ , thus the order  $n$  is most likely correctly determined. If  $n$  is decreased by one for each peak,  $T_0$  becomes about 41 minutes but the scatter is increased somewhat.

The largest peak at  $62.29 \mu\text{Hz}$  appears not to be consistent with the asymptotic formula with the  $T_0$  we have found. If the alternate choice of the  $62.29 \mu\text{Hz}$ - $73.84 \mu\text{Hz}$  pair were chosen, the largest peak would be at  $73.84 \mu\text{Hz}$  which would be identified as  $l=1, n=8$ . In this case a peak at  $50.7 \mu\text{Hz}$  shows up in the peak finding procedure and would be identified as  $l=2, n=20$ .

Note that in several cases two peaks have been assigned to one order  $n$  in the  $l=1$  series. These peaks have an average separation of  $1.2 \mu\text{Hz}$  and could be evidence of rotationally split modes. Assuming the  $l=1$  modes are  $m=\pm 1$ , the  $1.2 \mu\text{Hz}$  separation would correspond to a rotation rate  $\Omega = 7.5 \times 10^{-6} \text{sec}^{-1}$ . The rotational splitting kernel for these modes has a broad maximum between 0.2 and 0.5  $R$ . Assuming a smooth form for  $\Omega(r)$  as in Figure 2 of Gough (1982),  $J_2$  can be calculated and is of order  $1.7 \times 10^{-6}$ . This value differs from that found by Hill et al. (1982).

The sensitivity of the Stanford instrument to degree  $l=2$   $g$ -mode oscillations must be considered. For the previously reported acoustic mode oscillations in the 5-minute range, the Stanford velocity differencing scheme is most sensitive to modes of degree  $l=3$  to  $l=5$  but is not sensitive to modes of degree  $l=1$  or  $l=2$ . For low frequency  $g$ -modes, Gough and Cristensen-Dalsgaard (1982) have shown that for periods around 160 minutes the Stanford instrument is most sensitive to modes with degree  $l=5$  to  $l=7$ . For longer periods however, the instrument begins to be relatively more sensitive to modes with lower degree. This variation with period, unlike the case for the  $p$ -modes, is due to the importance of the horizontal motions induced by the internal gravity modes. To properly estimate the sensitivity to the various modes the oscillation energy must also be considered. In the simplest case, the combined effect of equipartition of energy between modes and the mode visibility with the Stanford instrument yields the greatest sensitivity for  $l=1$  and  $l=2$  at these longer periods.

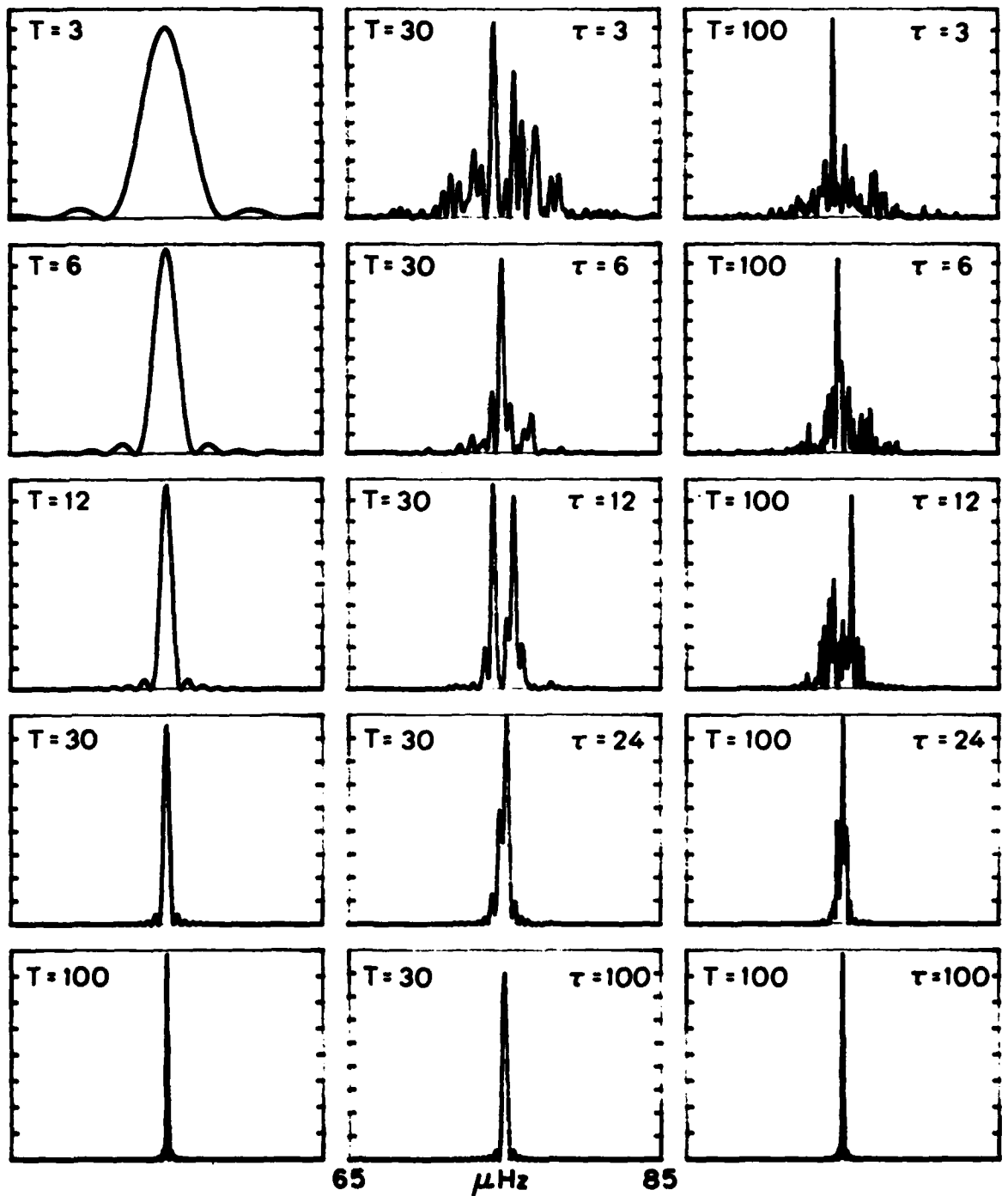


Figure 6. Artificial spectra computed from a single frequency signal with a selection of sample times and lifetimes. The sample duration  $T$  and mode lifetime  $\tau$  vary from 3 days to 100 days.

The theory predicts several hundred periods for low degree  $g$ -modes in the period interval examined. Only the most visible handful of peaks has been examined and has been found to be consistent with the theory. The relative peak sizes and simplicity of the analysis leads to the present mode identification. Alternative identifications are quite possible but they can only be tested with more data from other years or from other observatories.

#### *Note Concerning Lifetimes*

There are some general considerations concerning the appearance of power spectra of data containing oscillations of finite lifetime that must be remembered when interpreting such spectra. It is generally recognized that the spectrum of an oscillator with a lifetime  $\tau$  greater than the observation time  $T$  will be a "line" that will appear as a  $\text{sinc}^2$  with width  $1/T$ . It is also recognized that an observation of a single oscillation event with lifetime  $\tau$  and observation time  $T$  will result in a similar spectral line but with width  $1/\tau$ . What is sometimes forgotten is that if the observation duration includes several, but not many instances of an oscillation lifetime, i.e.  $T > \tau$  but not  $T \gg \tau$ , the spectrum will be a complex structure of lines of width  $1/T$  in an envelope of width  $1/\tau$ . If  $T \approx 2\tau$  the spectrum will look similar to that of a rotationally split  $l = 1$  mode. Figure 6 shows spectra computed from artificial data constructed with  $T = 3$ -days through  $T = 100$ -days and  $\tau = 3$  days through  $\tau \gg 100$  days. There were no data gaps assumed. The plot scales were adjusted such that the plots almost fill the frame. An examination of Figure 6 shows that caution must be used in interpreting spectra of oscillatory signals of unknown lifetimes.

#### *Acknowledgements.*

I thank Philippe Delache for acting as an ambassador of  $g$ -modes. His efforts have resulted in timely comparisons of results from the available sets of observations. This work was supported in part by the Office of Naval Research under Contract N00014-76-C-0207, by the National Aeronautics and Space Administration under Grant NGR05-020-559 and Contract NAS5-24420, by the Atmospheric Sciences Section of the National Science Foundation under Grant ATM77-20580 and by the Max C. Fleischmann Foundation.

#### *References.*

- Bath, Markus, *Spectral Analysis in Geophysics*, Elsevier Scientific Publ. Co., (1974).  
Berthomieu, G., J. Provost, and J. Christensen-Dalsgaard, (private communications).  
Christensen-Dalsgaard, J. and D.O. Gough, *Mon. Not. Roy. Astron. Soc.*, **198**, 141 (1982).  
Delache, P. and P.H. Scherrer, *Nature*, in press, (1983).  
Gough, D. O., *Nature*, **298**, 334, (1982).  
Hill, H. A., R. Bos, and P. R. Goode, *Phys. Rev. Lett.*, **49**, 1794, (1982).  
Scherrer, P.H., *Proceedings of the Study Conference "Oscillations as a Probe of the Sun's Interior"*, Catania, (submitted 1983).  
Scherrer, P.H., Wilcox, J.M., Kotov, V.A., Severny, A.B. and Tsap, T.T., *Nature*, **277**, 635-637 (1979).  
Scherrer, P.H., J.M. Wilcox, J. Christensen-Dalsgaard and D.O. Gough, *Solar Phys.* **82**, 75-87, (1983).  
Scherrer, P.H. and Wilcox, J.M., *Solar Phys.*, **82**, 37-42 (1983).  
Tassoul, M., *Astrophys. J. Suppl.*, **43**, 489-490 (1980).

**DAT  
FILM**